

The theoretical analysis and numerical simulation of the metal jet incoherence

Jun Liu^a and Zheng Wang

Institute of Applied Physics and Computational Mathematics, Beijing 100094, China

Abstract. By the analysis of the classic jet theory and literature, the regions of no-jet, convergent jet and incoherent jet are given in convergent point coordinate system. The theoretical analysis of metal jet incoherence formation explains Walker's jet incoherence theory which is based on experiment, and it's proved that in the supersonic portion of the metal jet, both the incoherence jet and the convergence jet can be formed. The jet incoherence estimation equation is given by our theoretical analysis. At last the numerical simulation of the copper jet formation process at different speeds and angles is done. The typical images of bifurcated jet, hollow jet and dense rarefaction jet are given by calculations to confirm the theoretical analysis results.

1. Introduction

Metal collision to form a shaped jet in low speed or supersonic conditions may have many complex physical phenomena, it may not produce metal jet or generate unsteady jet. In the study of metal shaped jet, Birkhoff put forward the classic jet theory. Pugh develop this theory, and puts forward the quasi-steady jet theory. But neither of the constant jet or the quasi-steady jet theory can correctly predict the conditions in which it can't form metal jet or generate unsteady jet. Because these theories are based on the incompressible fluid assumption.

In the process of metal shaped jet formation, the convergent metal jet is formed generally. Due to the shock wave blockade and strength blockade the metal jet may be not formed. In the incoherence jet conditions it can be divided to bifurcated jet and rarefaction jet. And the rarefaction jet can be divided into hollow jet and dense rarefaction jet. It is generally believed that the hollow jet will evolve into bifurcated jet in a long distance, but the dense rarefaction jet is different from the bifurcation jet.

Because the radial expansion of the metal jet will greatly reduce the penetration ability, the research of the incoherence jet formation is becoming a hot spot. Although the supersonic collision to form stable metal jet is possible, the incoherence jet phenomenon have been observed from experiments in the supersonic region. The assumption is proposed by Zhou [1] (θ_c is the limit angle to produce the attached shock wave):

- (1) In the subsonic flow collision, the convergent jet can be formed;
- (2) In the supersonic flow collision, if $\theta < \theta_c$, that will do not produce jet;
- (3) In the supersonic flow collision, if $\theta > \theta_c$, the incoherence jet is formed.

^a Corresponding author: caepcfd@126.com

Experiments show that the incoherence jet is effected by the material sound velocity. Walker [2,3] put forward the opposite view from Zhou: The incoherence of metal jet is not decided by the shock wave in supersonic collision, but the state in high pressure collision area is important for the convergent jet formation.

In this paper, the areas of no-jet, convergent jet and incoherent jet are given by the analysis of the classic jet theory in convergent point coordinate. And then, the Walker's incoherence jet theory is introduced and analyzed. As the supplement of Walker's theory, the metal jet incoherence is analysed in different supersonic speed ranges. At the end, the multi-material elastic-plastic hydrodynamic Euler method is used to simulate the metal jet incoherence phenomena. The simulation of the copper jet formation process at different speeds and angles is given to confirm our theoretical analysis results.

2. Theory of metal jet formation

In the metal shock blockade theory, the relationship between pressure p , density and velocity deflection angle θ_1 can be given by analysis of the physical characteristics between wave front and wave after. Combined with the Hugoniot relation and the equation of state, the $p - \theta$ polar curve of Cu is given in Fig. 3.

In the polar curve, θ_{max} is the max deflection angle to produce the attached shock wave at different initial velocity q_0 . And then the metal shock blockade curve can be computed (Fig. 4-L₁), the shock wave blockage area is the region below this curve in where there is no jet formation.

The strength blockade theory is based on ideal elastoplastic assumption, it's considered that The normal velocity q_{\perp} must be greater than the material strength Y_0 to form the metal jet. So the critical angle of the strength

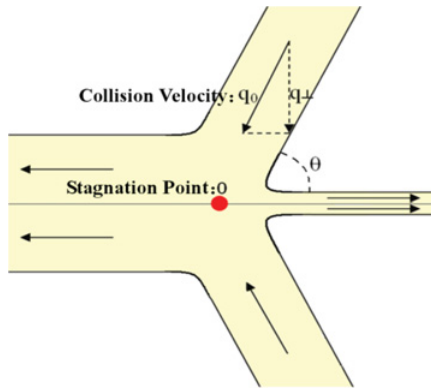


Figure 1. The metal jet formation in convergent point coordinate system (q_0 is collision velocity, θ is collision angle, O is stagnation point.)

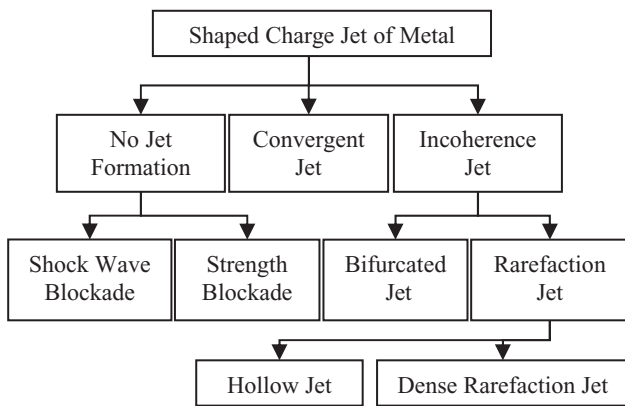


Figure 2. The classification of the shaped charge jet.

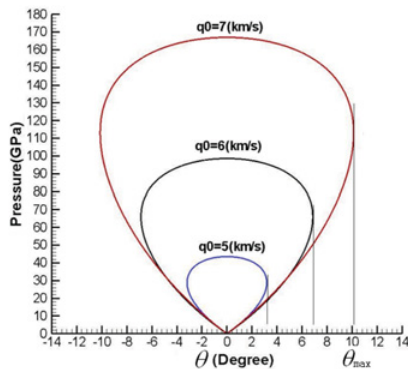


Figure 3. The pressure-angle polar curve of copper using Mie-Grüneisen equation of state.

blockade θ_2 is defined as

$$\sin \theta_2 = \frac{1}{q_0} \sqrt{\frac{2Y_0}{\rho}} \quad (1)$$

the metal strength blockade curve is computed (Fig. 4-L₂), and if $\theta < \theta_2$, there is no jet formation.

The metal jet incoherence experiment indicates that the convergent jet can be formed when the collapse velocity is less than 1.23 times the body sound speed in copper

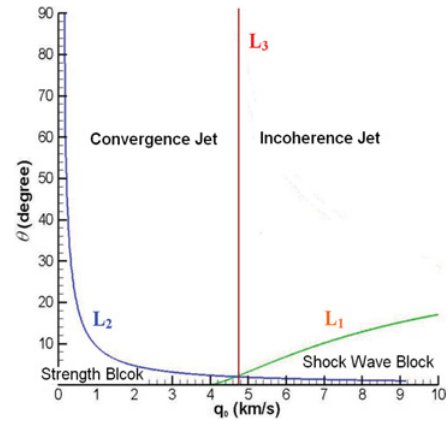


Figure 4. The region of no-jet, convergent jet and incoherent jet of copper in convergent point coordinate.

shaped cover. By extending this criterion to other shaped cover materials, Walker [2] give out the criterion below:

- (1) In the convergent point coordinate, if $q_0 > C_L$, the bifurcated jet or discontinuous jet is formed;
- (2) In the convergent point coordinate, if $q_0 < C_L$, the convergent jet is formed;
- (3) In the convergent point coordinate, if $q_0 \approx C_L$, the hollow jet is formed;

C_L is the low longitudinal wave velocity, it's defined as:

$$C_L = \sqrt{3 \frac{1-\gamma}{1+\gamma}} C_0, \quad C_0 = \sqrt{\frac{K}{\rho}} \quad (2)$$

γ is the poisson coefficient, K is the bulk modulus. So the metal jet incoherence curve is given by Fig. 4-L₃ which identify the jet incoherence region.

Cu: $\gamma = 0.35$, $C_L = 1.20C_0$; Fe: $\gamma = 0.29$, $C_L = 1.28C_0$; Ni: $\gamma = 0.30$, $C_L = 1.27C_0$. These data are very close to the experimental results of copper: $q_{\perp} = 1.23C_0$. Therefore, using the 1.23 multiplier for other materials as the jet incoherence criterion seems to be reasonable. However, the jet formation process is very complex. In the shaped cover collapse before flying to convergent point, it has experienced a shock loading and unloading expansion. Therefore, in the dynamic convergence collision it is not the original state, especially the collision area has a higher pressure. In 1996, Walker [3] reiterated that using the volume velocity is more reasonable, and the experimental factor 1.23 may not equal to C_L/C_0 . Note that Walker's analysis of jet incoherence theory is not perfect, we give a demonstration of the jet incoherence theory in the convergent point coordinates, to verify the Walker's experimental criterion.

3. Theoretical analysis of the metal jet incoherence

Two metal rod with infinite length and limited width collide at a certain angle and speed. We can only analyse the upper half part because of the symmetry. Define the upstream density, stream tube width and velocity is ρ_0, A_0, \vec{q}_0 in a stream tube l_1 which do not close to

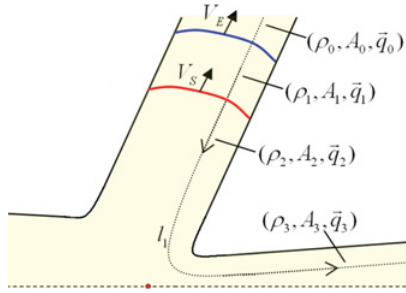


Figure 5. The formation of metal-collision jet and the position of shock wave.

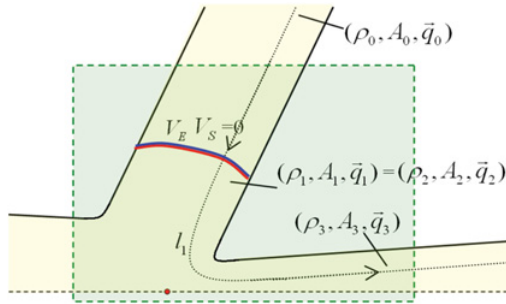


Figure 6. The region of steady flow when $|\vec{q}_0| > C_L$.

the outer surface; behind the elastic longitudinal wave, the density, stream tube width and velocity is ρ_1, A_1, \vec{q}_1 ; behind the body wave, the density, stream tube width and velocity is ρ_2, A_2, \vec{q}_2 ; after crossing through the high pressure area and unloading to zero pressure condition, the density, stream tube width and velocity is ρ_3, A_3, \vec{q}_3 . The velocity of the elastic longitudinal wave is V_E , and the velocity of the body wave is V_S .

It's intuitively considered that the judgment of the jet incoherence is: if $A_3 > A_0$, the metal jet is incoherence; if $A_3 \leq A_0$, the metal jet is convergent. The initial velocity range is divided into two kinds of situations: $|\vec{q}_0| > C_L$ and $C_0 < |\vec{q}_0| < C_L$.

$$(1) \quad |\vec{q}_0| > C_L.$$

In this condition, the position of the elastic longitudinal wave and body wave is not moved ($|V_E| = |V_S| = 0$). The process of upstream area unloading to zero pressure area can be seemed as a steady flow.

In an ideal without heat conduction, Bernoulli integration can be done in steady region along the streamline:

$$\frac{\vec{q}^2}{2} + e + \frac{p}{\rho} + \tilde{V} = C(\psi) \quad (3)$$

$C(\psi)$ is the function of streamline number ψ (in uniform stream, $C(\psi)$ is a constant). In this model $\tilde{V} = 0$, along the streamline we can get:

$$\frac{\vec{q}_0^2}{2} + e_0 + \frac{p_0}{\rho_0} = \frac{\vec{q}_3^2}{2} + e_3 + \frac{p_3}{\rho_3}. \quad (4)$$

The upstream state have $p_0 = 0, e_0 = 0$. If the density does not change with temperature, the state unloading to zero

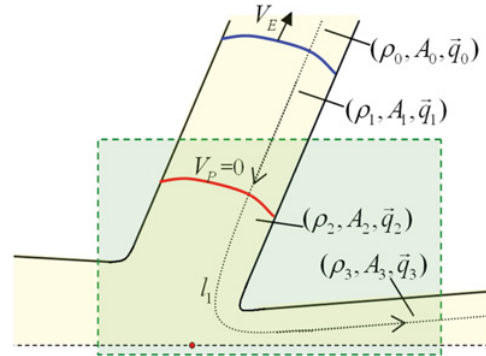


Figure 7. The region of steady flow at $C_0 < |\vec{q}_0| < C_L$.

pressure area have $p_3 = 0, \rho_3 = \rho_0, e_3 > 0$. Get into (4):

$$|\vec{q}_0| > |\vec{q}_3|. \quad (5)$$

Combine with the conservation of mass ($\rho_0 |\vec{q}_0| A_0 = \rho_3 |\vec{q}_3| A_3$), we can get:

$$A_0 < A_3. \quad (6)$$

This analysis result show that the metal jet is incoherence when $|\vec{q}_0| > C_L$, and it's the same as Walker's experimental results.

$$(2) \quad C_0 < |\vec{q}_0| < C_L.$$

In this condition, the position of body wave is not moved ($|V_S| = 0$), but the elastic longitudinal wave velocity is not zero ($|V_E| > 0$). The process from behind elastic longitudinal wave area to unloading to zero pressure area can be seemed as a steady flow.

The elastic wave velocity is $D = C_L - |\vec{q}_0|$, the shock wave relations is:

$$\begin{aligned} \rho_1(D - |\vec{q}_1|) &= \rho_0(D - |\vec{q}_0|) \\ \rho_1(D - |\vec{q}_1|)^2 + p_1 &= \rho_0(D - |\vec{q}_0|)^2 + p_0 \quad (7) \\ e_1 + \frac{p_1}{\rho_1} + \frac{(D - |\vec{q}_1|)^2}{2} &= e_0 + \frac{p_0}{\rho_0} + \frac{(D - |\vec{q}_0|)^2}{2} \end{aligned}$$

We use the state equation below to simplify analyzing:

$$p = (\gamma - 1)\rho e + C_0^2(\rho - \rho_0). \quad (8)$$

By Bernoulli integration (3), along the streamline we can get:

$$\frac{\vec{q}_1^2}{2} + e_1 + \frac{p_1}{\rho_1} = \frac{\vec{q}_3^2}{2} + e_3 + \frac{p_3}{\rho_3}. \quad (9)$$

In this place, we also have $p_3 = 0, \rho_3 = \rho_0$. On the simultaneous (7), (8) and (9):

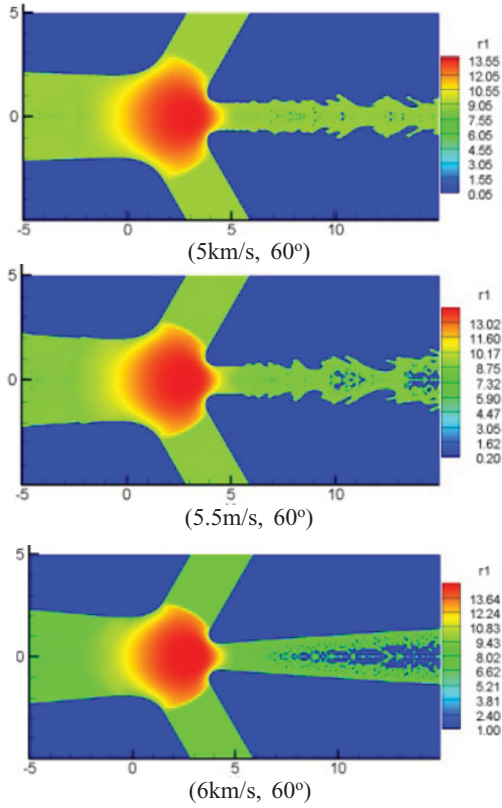
$$\frac{\vec{q}_3^2}{2} = \frac{\vec{q}_0^2}{2} + \left(\frac{2(C_L - \vec{q}_0)(C_L^2 - C_0^2)}{C_L(\gamma + 1)} - e_3 \right) \quad (10)$$

By the conservation of mass ($\rho_0 |\vec{q}_0| A_0 = \rho_3 |\vec{q}_3| A_3$), we can get:

$$\begin{aligned} \frac{A_0^2}{A_3^2} &= 1 + \frac{2}{\vec{q}_0^2} Q, \\ Q &= \frac{2(C_L - \vec{q}_0)(C_L^2 - C_0^2)}{C_L(\gamma + 1)} - e_3. \end{aligned} \quad (11)$$

Table 1. The parameters of constitutive equations and state equation of copper.

Constitutive Equation		Equation of State	
Y_0 (GPa)	0.12	ρ_0 (g/cm ³)	8.93
Y_{max} (GPa)	0.64	γ_0	1.99
β	36	C_0 (km/s)	3.94
n	0.45	S_1	1.489
b (GPa ⁻¹)	0.028	S_2	0
h (K ⁻¹)	3.8e-4	S_3	0
T_{m0} (K)	1790	a	0.47
ε_{00}	-0.1178	P_{min} (GPa)	1.8
ε_{01}	-0.2344		
ε_{02}	7.529		
ε_{03}	15.26		
ε_{04}	21.90		
R (kJ/g/K)	1.3d-4		

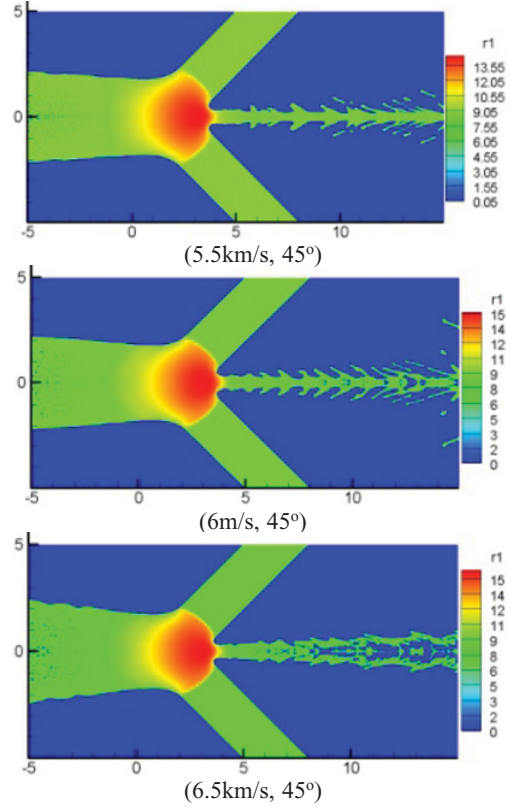

Figure 8. The density image at 60° with different collision velocity.

So, the positive or negative of Q determine whether the metal jet is incoherence or not in $C_0 < |\vec{q}_0| < C_L$:

- (1) if $Q < 0$, the metal jet is convergence;
- (2) if $Q > 0$, the metal jet is incoherence.

In the Eq. (11), if $|\vec{q}_0| \geq C_L$, $Q < 0$, the incoherence jet is formed, this result is just the same as analysis in previous section.

When $C_0 < |\vec{q}_0| < C_L$, the metal jet may be complex, it does not follow Walker's analysis. According to our theoretical analysis, the incoherence situation can be evaluated by Eq. (14).


Figure 9. The density image at 45° with different collision velocity.

4. Numerical simulation of metal jet incoherence

The multi-material elastic-plastic hydrodynamic Euler program "MEPH" [4,5] is used to simulate the metal jet incoherence phenomena. The Steinberg-Guinan constitutive model is used:

$$G = G_0 \left[1 + bp \cdot \left(\frac{\rho}{\rho_0} \right)^{1/3} - h(T - 300) \right]$$

$$Y = Y_0 (1 + \beta \varepsilon^p)^n \left[1 + bp \cdot \left(\frac{\rho}{\rho_0} \right)^{1/3} - h(T - 300) \right]$$

$$Y_0 (1 + \beta \varepsilon^p)^n \leq Y_{max} \quad (12)$$

$$T = (E - \varepsilon_0) / 3R,$$

$$\varepsilon_0 = \varepsilon_{00} + \varepsilon_{01}x + \varepsilon_{02}x^2 + \varepsilon_{03}x^3 + \varepsilon_{04}x^4, \quad x = 1 - \rho_0/\rho$$

$$T_m = T_{m0} \left(\frac{\rho_0}{\rho} \right)^{2/3} \exp[2\gamma_0(1 - V)].$$

Mie-Gruneisen state equation is used:

$$p = \rho_0 c^2 \mu \frac{\left[1 + (1 - \frac{\gamma_0}{2})\mu - \frac{a}{2}\mu^2 \right]}{\left[1 - (S_1 - 1)\mu - \frac{S_2\mu^2}{(\mu+1)} - \frac{S_3\mu^3}{(\mu+1)^2} \right]^2}$$

$$+ (\gamma_0 + a\mu)E, \quad (13)$$

$$\mu = \frac{\rho}{\rho_0 - 1}.$$

The simulations with different collision velocity is done under $\theta=60^\circ, 45^\circ$.

In the Fig. 8 and Fig. 9, the collision velocity is bigger than 1.23 times the speed of the body sound, the simulation results show that copper jet is incoherence. And with the increase of the stream velocity, the copper jet incoherence forms is evolved from hollow jet to bifurcation jet gradually. With the decrease of collision angle, the hollow jet and bifurcation jet is formed more difficultly.

5. Summary

In this paper, the classical jet theory is reviewed, and the regions of no-jet, convergent jet and incoherent jet are given in convergent point coordinate. The metal jet incoherence is analyzed in different supersonic speed ranges: when $|\vec{q}_0| > C_L$ the metal jet must be incoherence; but when $C_0 < |\vec{q}_0| < C_L$ the metal jet forms are complex, either incoherence jet or convergence jet may be formed. And the jet incoherence judgment equation is given by our theoretical analysis In $C_0 < |\vec{q}_0| < C_L$. At the end,

both the dense rarefaction jet, hollow jet and bifurcation jet is simulated to verify the correctness of the theoretical analysis. Jet incoherence theory research and its numerical simulation can be widely applied in shaped charge jet, high-velocity impact and micro-jet formation.

The first author was supported by NNSF(11371069, 11371065, 11372052).

References

- [1] Pei Chi Chou, Joseph Carleone, Robert R. Karpp, J. Appl. Phys., **47**, 7: 2975–2981 (1976)
- [2] Walker J.D., *14th International Symposium on Ballistics*, 165–172 (1993)
- [3] Walker J.D., *16th International symposium on Ballistics*, 457–462 (1996)
- [4] He C J, Yu Z L, Feng Q J, Chinese Journal of Explosion and Shock Waves, **19**, 3: 216–221 (1999)
- [5] Liu Jun, He C J, Liang X H. Chinese Journal of High Pressure Physics, **22**: 72–78 (2008)